Working title

Shifts from pulled to pushed range expansions caused by reductions in connectedness

Authors

Maxime Dahirel[1], Aline Bertin[1], Marjorie Haond[1], Aurélie Blin[1], Eric Lombaert[1], Vincent Calcagno[1], Simon Fellous[2], Ludovic Mailleret[1], Elodie Vercken[1]

[1]INRAE, Université Côte d'Azur, CNRS, ISA, France

[2]INRAE, Univ. Montpellier, CIRAD, IRD, Montpellier SupAgro, CBGP, France

Corresponding author: MD, maxime.dahirel@yahoo.fr

Abstract

While species ranges have always moved, the ecological and evolutionary dynamics of range expansions have become especially relevant today, as human influence reshapes ecosystems worldwide. As a consequence, there have been many attempts to explain and predict evolutionary and demographic dynamics observed during range expansions. However, many of these predictions are based, explicitly or implicitly, on a subset of possible range expansion types, so-called "pulled" dynamics, in which the low-density front populations provide most of the "fuel" for the advance. Some expansions may exhibit very different dynamics, with high-density populations behind the front "pushing" the expansion forward. Studying the ecological and evolutionary consequences of pushed vs. pulled dynamics remains challenging, due to difficulties in reliably generating or identifying pushed and pulled waves in experimental or natural settings. Manipulations of the within-habitat quality to create Allee effects have successfully created pushed waves, but may only be applicable in some contexts. We here propose that manipulating, and specifically reducing the degree of structural connectivity among habitats may prove a more generalizable way to create pushed waves, through density-dependent dispersal. We demonstrate this using both individual-based simulations as well as replicated experimental range expansions (with the parasitoid wasp *Trichogramma brassicae* as model). Analysing expansion velocities and neutral genetic diversity, we showed that restricting connectivity did lead to pushed dynamics. Interestingly, our results suggest that reducing connectivity led to density-dependent spread (and thus pushed waves) through two different mechanisms in simulated and experimental expansions. In the current context of habitat loss and fragmentation, we need to better account for this relationship between connectedness and expansion regimes to be able to successfully predict the ecological and especially evolutionary consequences of range expansions.

Keywords Allee effects, biological invasions, density-dependent dispersal, individual-based model, range expansions, range shifts, *Trichogramma*

Introduction

Range expansions and range shifts into novel habitats and landscapes are key ecological processes shaping the abundance and distribution of species (Sexton, McIntyre, Angert, & Rice, 2009). Understanding their ecological and evolutionary drivers and consequences has become especially relevant in the context of ever-increasing biological invasions (Facon et al., 2006; Renault, Laparie, McCauley, & Bonte, 2018) or species responses to climate change (Hill, Griffiths, & Thomas, 2011; Lavergne, Mouquet, Thuiller, & Ronce, 2010; Parmesan, 2006).

Range expansions are usually modelled as travelling waves, and analysed in a framework based on the Fisher-KPP equation and the numerous works that derive from it (see e.g. Hastings et al., 2005; Lewis, Petrovskii, & Potts, 2016). In this framework, waves are considered "pulled" when spread is driven mostly, if not only, by the dynamics at the leading edge of the expansion. In biological range expansions, this happens when growth and dispersal are maximal at low densities; the velocity of the wave then only depends on low-density dispersal and growth (e.g. Birzu, Matin, Hallatschek, & Korolev, 2019). While growth- and dispersal-density reaction norms expected to generate pulled waves do happen in nature (Harman, Ii, Shivaji, & Cronin, 2020; Matthysen, 2005; Williams & Levine, 2018), they are likely not the rule. Indeed, dispersal is often maximised at high densities instead (positive density-dependence) as it provides a mechanism to escape increased competition (Bowler & Benton, 2005; Harman et al., 2020; Matthysen, 2005). Additionally, growth rates can be reduced at low densities compared to intermediate ones, a phenomenon known as the Allee effect (Berec, Angulo, & Courchamp, 2007). In both cases, we would expect the advance of the expansion wave not to be driven by the low-density front populations, but by population dynamics in a region located behind the front and where growth and/or dispersal are maximal. These "pushed" waves (Stokes, 1976) may behave very differently than pulled waves (see e.g. Lewis et al., 2016). They will typically advance faster than expected based solely on their low-density growth and dispersal rates; though, the distinction is important, not necessarily faster (and often slower) than pulled waves with the same *average* growth and dispersal (see e.g. Gandhi, Korolev, & Gore, 2019). The ratio of the actual front velocity v to the so-called "Fisherian" velocity v_F expected for a pulled wave with the same low-density behaviour has been proposed as a quantitative indicator separating pulled, "semi-pushed" and pushed waves (e.g. Birzu, Hallatschek, & Korolev, 2018). This ratio is connected to other key metrics expected to vary along the pushed/pulled gradient (Birzu et al., 2018). In the context of biological range expansions or invasions, this includes the rate at which the front of the wave loses genetic diversity due to drift and successive founding events during expansions. Indeed, models and experiments show that neutral genetic diversity is lost at the front much more slowly in pushed waves than in pulled waves (Birzu et al., 2018, 2019; Gandhi et al., 2019; Hallatschek & Nelson, 2008;

Roques, Garnier, Hamel, & Klein, 2012), with estimated times to allele fixation differing by up to several orders of magnitude (Gandhi et al., 2019).

A key challenge for empirically studying the ecological and evolutionary consequences of pushed and pulled waves (which, besides neutral genetic diversity, remain poorly known; see discussion in Birzu et al., 2019) is to obtain comparable expansions known to be either pushed or pulled. One could compare strains, populations or closely related species naturally differing in the intensity of density-dependent dispersal and/or Allee effects (Harman et al., 2020; Jacob, Chaine, Huet, Clobert, & Legrand, 2019; Matthysen, 2005; Walter, Grayson, Blackburn, Tobin, & Johnson, 2019). However, they are likely to also differ in other key traits (Jacob et al., 2019), making direct comparisons difficult. A better experimental solution would be to manipulate the focal species/population/strain's environment to change the presence or strength of Allee effects and/or density-dependent dispersal. For instance, Gandhi et al. (2019; 2016) managed to reliably produce pushed waves by changing the substrate on which *Saccharomyces cerevisiae* yeasts were grown: while yeasts grow best at low densities on monosaccharides, they present an Allee effect when they have to use a disaccharide like sucrose. Externally manipulating density-dependent dispersal may be more difficult, but could conceivably also be done by changing the resource (Endriss et al., 2019; Kuefler, Avgar, & Fryxell, 2012; Van Allen & Bhavsar, 2014). Adding or removing conspecific cues while keeping the actual population constant may also be an option (De Meester & Bonte, 2010).

Rather than manipulating the within-habitat/patch conditions, another solution that may be more generalizable (as not all organisms have resources or cues that are easy and useful to manipulate experimentally) would be to restrict the level of connectedness (i.e. structural connectivity; Baudry & Merriam, 1987) between patches/populations. We hypothesize such experimental manipulations could lead to increased positive density-dependent dispersal, and thus more pushed waves, because of dispersal stochasticity. Indeed, at low population sizes, reducing the dispersal rate by limiting connectedness sharply increases the risk some populations will fail to send any disperser, due to stochasticity alone (**Fig. 1**). We predict this can lead to a positive, if non-linear, relationship between spread and population density. The densities at which we expect this mechanism to be relevant are not uncommon in nature, but very low based on the range most models use, which may explain why it has been overlooked so far (compare natural population densities in Krauss, Steffan-Dewenter, & Tscharntke, 2003; Minto, Myers, & Blanchard, 2008; Santini, Isaac, & Ficetola, 2018; Stephens, Vieira, Willis, & Carbone, 2019; with densities in Birzu et al., 2018; or Gandhi et al., 2019; for instance). Besides, models have often assumed continuous population densities instead of discrete individuals, which prevent the phenomenon described in **Fig. 1** from occurring (as discussed in Pachepsky & Levine, 2011). An indication this mechanism may work and generate pushed waves can be found in

105 an earlier simulation study by Morel-Journel et al. (2016). In that study, increasing the level of
106 dispersal stochasticity led to levels of within-landscape population variability more closely resembling
107 simulated pushed waves than pulled waves.

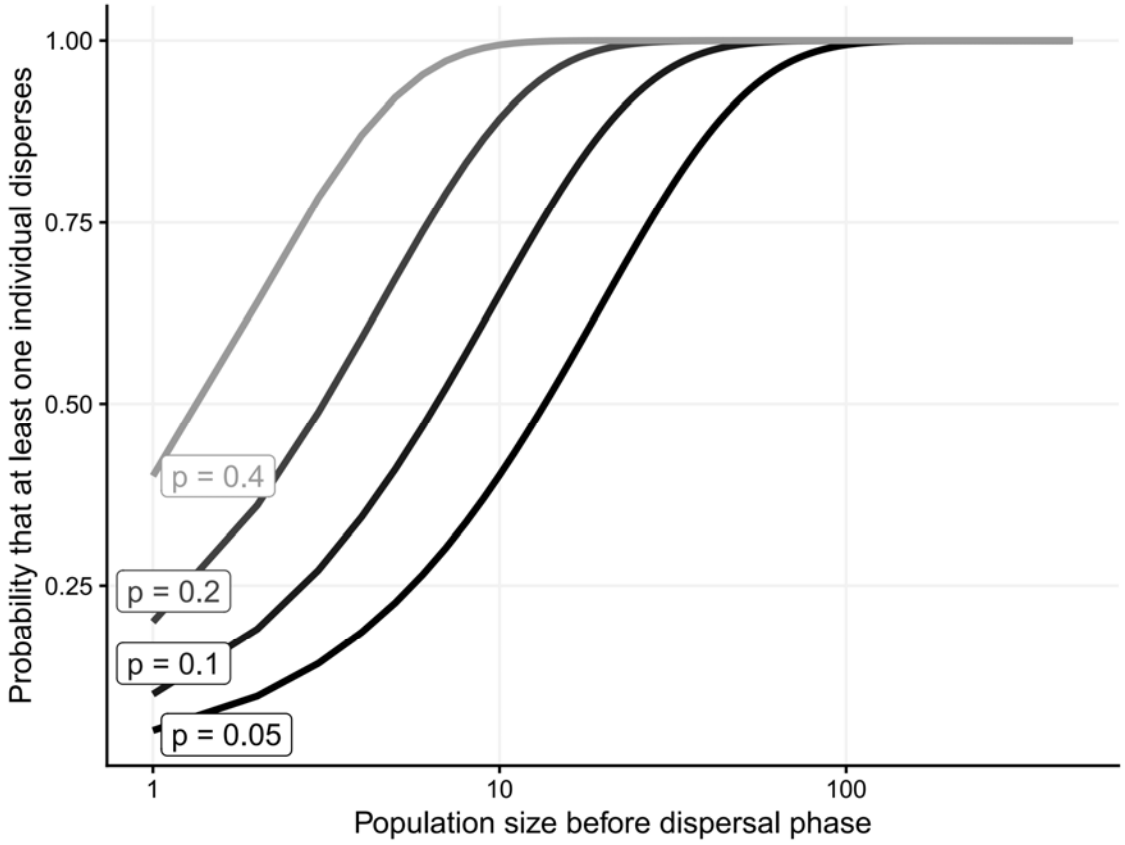

108

109 **Figure 1.** Probability that at least one individual disperses from a patch (Pr(n>0)) as a function of its
110 population size N pre-dispersal and average dispersal rate p. Dispersal stochasticity is obtained by
111 assuming the number of dispersers n from a patch is drawn from a Binomial distribution
112 n=Binom(N,p). Note the log scale on the x-axis.

113

114 **In the present study, we aimed to demonstrate, combining simulations and experimental**
115 **approaches, that pushed waves can indeed arise from reductions of habitat connectedness**, at
116 population densities that are realistic for many "macroscopic" organisms. In individual-based
117 simulations, we examined expansion velocities and the dynamics of neutral genetic diversity to (a)
118 confirm Allee effects and density-dependent dispersal (Birzu et al., 2019) still lead to pushed waves
119 at "low" equilibrium population sizes K, and (b) show that reducing connectedness (by decreasing
120 effective dispersal rates) can also generate pushed fronts. We then used minute wasps of the
121 *Trichogramma* genus (Haond et al., 2018; Morel-Journel et al., 2016), and replicated experimental

landscapes (Larsen & Hargreaves, 2020), to investigate whether reduced connectivity influenced the velocity and neutral genetic dynamics of empirical range expansions.

Methods

Study species

We used laboratory strains of the egg parasitoid *Trichogramma brassicae* Bezdenko, 1968 (Hymenoptera: Trichogrammatidae) as our model in experiments (**Supplementary Material 1**). *T. brassicae* wasps are raised routinely in the lab using eggs of the Mediterranean flour moth *Ephestia kuehniella* Zeller 1879 (Lepidoptera: Pyralidae) as substitution host. *E. kuehniella* eggs are irradiated before use, which prevents their larval development while still allowing *Trichogramma* wasps to use them as hosts (St-Onge, Cormier, Todorova, & Lucas, 2014). To be able to better generalize our results, we used three independent genetic mixes of *T. brassicae* (**Supplementary Material 1**). Note that the effect of genetic background itself is not the object of the present manuscript, and is thus not analyzed directly in any of our statistical models, for simplicity (as in Van Petegem et al., 2018).

Experimental landscapes and range expansions

To experimentally test the effects of reduced connectivity on range expansions, we set up a series of artificial landscapes in which we monitored *T. brassicae* wasps for 14 non-overlapping generations (including initially released adults, i.e. generation 0). The one-dimensional landscapes were made of closed plastic vials (5 cm diameter, 10 cm height) connected by either two ("reference"-level connectedness) or one (restricted connectedness) flexible tubes to each of their nearest neighbours (tube length: 40 cm, internal diameter: 5 mm). Each treatment was replicated 12 times (4 per genetic mix), for a total of 24 experimental landscapes. Landscapes were initiated by introducing ≈ 300 adult wasps (range 261 – 324) in one extremity patch (x = 0), so the front could expand in only one direction in each landscape. Landscapes were kept under standardized conditions (23°C, 70% relative humidity, 16:8 L:D). Each generation then unfolded along the following steps:

- (a) We provided approximately 450 new eggs of *Ephestia kuehniella* per patch for wasps to lay eggs in. *E. kuehniella* eggs were presented on paper strips to facilitate handling.

- (b) Adults were removed after 48 hours to enforce non-overlapping generations and standardized generation times.

- (c) When parasitoid larval development was advanced enough to result in visible darkening (after 7 days), we temporarily removed egg strips from patches and assessed the presence/ absence of parasitized eggs by eye. We also photographed all patches with parasitized eggs for estimations of

153 population sizes (Nikon D750 60mm f/2.8D macro lens, 24.3 Mpix, **Supplementary Material 2**). Eggs
154 were then replaced in their patches.

155 - (d) Finally, once adult wasps had emerged, old egg strips were removed and replaced with fresh
156 ones in each patch for the next generation. Landscapes, which were initially 4 patches long, were
157 extended as needed to ensure there were always at least 2 available empty patches beyond the
158 current front.

159 We validated the experimental design by comparing the estimated mean egg-laying distances (in
160 patches from release sites) between treatments at the start of the experiment, i.e. the only time
161 point when the source patch of all egg-laying individuals was known. Eggs were indeed laid on
162 average closer to the release site in "restricted connectedness" landscapes than in "reference" ones
163 (**Supplementary Material 2 and 3**).

164 *Microsatellite genotyping*

165 To understand how genetic diversity evolved during range expansions and whether it was influenced
166 by connectedness, we kept and genotyped some of the adult female wasps after their removal from
167 the experimental landscapes, using 19 microsatellite markers. In each landscape, we sampled initially
168 released individuals (i.e. generation 0; hereafter "origin" wasps) as well as wasps found in both the
169 release patch (hereafter "core" wasps) and the most advanced population ("front" wasps) at
170 generations 4, 8 and 12. In each population × time combination, we aimed to sample about 20
171 individuals; the actual number was sometimes lower especially in front populations with fewer
172 individuals (average ± SD: 18.12 ± 2.62 wasps; range: 4-28; total: 3044).

173 *Individual-based model*

174 To confirm that mechanisms previously shown to lead to pushed waves still do so at "low"
175 population sizes, and to determine whether the new mechanism we propose, reduced
176 connectedness, also generates pushed waves, we used an individual-based model (IBM) approach
177 (DeAngelis & Mooij, 2005 for a review). The model is in discrete time and space and simulates the
178 dynamics of a haploid clonal species with non-overlapping generations. Range expansions unfold
179 during 100 generations in a one-dimensional landscape long enough they never run out of empty
180 patches to expand to. In practice, given the expansions advance in only one direction and individuals
181 can only disperse at most one patch per generation (see below), this means any length higher than
182 the number of generations. All patches are of equal and constant quality, determined by the
183 equilibrium population density K. In the present study, we studied two K, 450 and 225, corresponding
184 respectively to 100% and 50% of the largest possible population in the experiment.

At the start of the expansion, K adult individuals that have not yet reproduced are introduced in one patch (x = 0) at one of the two extremities of the landscape, so the front could expand in only one direction. All individuals are randomly assigned one of two allele values (coded 0 and 1) at a neutral genetic locus L. Each generation until the end of a run, the life cycle then happens as follows:

(1) Adult individuals disperse following a Bernoulli distribution with a probability $D = logit^{-1}\left(logit(D_0) + \beta_{density} \times {}^{N}/_{K}\right)$, where D_0 is the (hypothetical) dispersal rate at N = 0, $\beta_{density}$ the slope of the dispersal-density relationship on the logit scale, and N the patch population size immediately before the dispersal phase. While this function may not be as optimal, in terms of fitness payoffs, as others described in the theoretical literature (Hovestadt, Kubisch, & Poethke, 2010), it is simpler (only 2 parameters) and is closer to the way empirical dispersal-density data are usually analysed (through GLMs; see e.g. Marjamäki, Contasti, Coulson, & McLoughlin, 2013). Dispersers randomly move to one of the nearest neighbours; that is, the maximal dispersal distance is 1.

(2) Individuals then produce F offspring, with $F \sim \mathrm{Poisson}(\lambda)$ and λ based on a Ricker equation modified to allow potential Allee effects (Morel-Journel et al., 2016): $\lambda = e^{r_0(1-{}^{N}/_{K})(1-{}^{A}/_{N})}$ where r_0 is the hypothetical expected growth rate at N = 0 in the absence of Allee effects, and A an Allee threshold such that A = 0 leads to no Allee effects, $0<A\leq 1$ leads to weak Allee effects (*sensu* e.g. Berec et al., 2007, i.e. where positive density-dependent growth never leads to negative growth rates), and $A > 1$ leads to strong Allee effects (where growth rates are negative for $N < A$). There are no mutations, meaning all new individuals inherit the value at the neutral locus L from their parent.

(3) All adults die; juveniles born in (2) then become adults.

The model was written in Netlogo (Wilensky, 1999), version 6.1.1, and set up using the *nlrx* R package (Salecker, Sciaini, Meyer, & Wiegand, 2019). We tested 4 scenarios (× 2 possible values of K; see **Table 1**). The "reference" scenario had no Allee effects, no density-dependent dispersal and a dispersal rate D_0 set to 0.2, a not unusual rate based on many experimental (e.g. Emanuel A. Fronhofer et al., 2018) or natural situations (Marjamäki et al., 2013; Stevens et al., 2013). The three other scenarios, which we expected to lead to pushed waves, each differed from the reference by one parameter: either a weak Allee effect was present (A = 0.95), there was positive-density-dependent dispersal ($\beta_{density}$ = 1) or connectivity was reduced by half (D_0 = 0.1). In all cases r_0 was set to ln(5), which is in the lower half of the range of values expected for *Trichogramma brassicae* wasps on *Ephestia kuehniella* eggs, given their fecundity, emergence rate and sex-ratio in experimental

settings (see e.g. Cerutti & Bigler, 1995) and assuming a reproductive period of 24 to 48 hours. Each scenario was replicated 100 times.

Statistical analyses

All data were analyzed in a Bayesian framework, using R, version 3.6.3 (R Core Team, 2020) and the *brms* package version 2.11.1 (Bürkner, 2017) as frontends to the Stan language (RStan version 2.19.2; Carpenter et al., 2017; Stan Development Team, 2018). We used nonlinear multilevel/mixed models. The model descriptions below are summaries aiming for clarity rather than completeness; formal and complete write-ups for all statistical models are given in **Supplementary Material 4**. We use general-purpose "weakly informative" priors based on McElreath (2020) for all parameters except one (logit(V_{max})), where there is strong theoretical prior knowledge (see **Supplementary Material 4**). For each model, we ran four chains with enough iterations to ensure effective sizes were satisfactory for all fixed effect, random effect and distributional parameters (both bulk- and tail-ESS *sensu* Vehtari, Gelman, Simpson, Carpenter, & Bürkner, 2020 > 1000). In addition to graphical posterior checks (Gabry, Simpson, Vehtari, Betancourt, & Gelman, 2019; Vehtari et al., 2020), we checked chain convergence using the improved $\widehat{R}$ statistic by Vehtari et al. (2020). All credible intervals given in text and figures are 95% Higher posterior Density Intervals (HDIs). Data handling and figure generation were mainly done using the various *tidyverse* packages (Wickham et al., 2019), as well as the *tidybayes* (Kay, 2019) and *patchwork* (Pedersen, 2019) packages.

<u>- Genetic diversity</u>

When expected heterozygosity (Nei, 1973) H is used as a measure of genetic diversity, theory predicts genetic diversity of a population should decay exponentially with time t during range expansions (Birzu et al., 2018; Hallatschek & Nelson, 2008):

$$H_t \sim H_0 . e^{-\lambda_{[g]} t}$$

, where H_0 is the initial heterozygosity, and $\lambda_{[g]}$ the rate of decay of genetic diversity. For experimental data, we used this equation directly in a non-linear model to estimate whether the dynamics of genetic diversity varied between our two treatments and between core and front patches. Multilocus expected heterozygosity was first calculated for each population × time combination using microsatellite data and the *adegenet* package (Jombart, 2008). Our submodel for $\lambda_{[g]}$ included fixed effects for treatment, location (initial release patch for "core"/ most advanced patch for "front") and their interactions, as well as a random effect of replicate identity. The submodel for the initial

diversity H_0 only included the random effect of replicate, as we did not expect differences between treatments beyond random fluctuations, and core/front patches are the same at t = 0. The effect of location in the $\lambda_{[g]}$ submodel was centred (-0.5 for "core", 0.5 for "front") and set to 0 at t = 0 as, again, core/front patches are the same at t = 0. The submodels were estimated on logit(H_0) and $\log_{10}(\lambda_{[g]})$ to keep them within proper bounds; expected heterozygosities are proportions, and the decay rate $\lambda_{[g]}$ must be positive. We fitted the overall model on logit(H_t) using a Student t distribution, rather than on H_t using a Beta distribution (and a logit link). This is because the former is likely to be more robust to rare outliers (Kruschke, 2015), like those caused by sampling effects before genotyping (see companion script for more detailed model comparisons, **Data availability**).

With simulated data, we cannot use the same equation as our basis to fit a model. This is because the way we simulate neutral genetic diversity (one locus with only two alleles in a haploid species) means values of H_t = 0 are very frequent (especially as t increases), and our previous model cannot be fitted to data containing zeroes. We instead used the fact that, with two alleles and if a given treatment is replicated a large number of times, a version of $\lambda_{[g]}$ can also be recovered from the way among-replicate variance in allelic frequencies V (for either allele) changes with time (Gandhi et al., 2019):

$$V_t \sim V_{max} \cdot (1 - e^{-\lambda_{[g]} t})$$

, where V_{max} is both the product of initial allelic frequencies and the asymptotic variance reached when all replicates have fixed one of the alleles. As for experimental data, our submodel for $\log_{10}(\lambda_{[g]})$ included fixed effects for treatment, location (core/front) and their interactions. The submodel for logit(V_{max}) included only a constant intercept, as V_{max} should be identical between all cases (and ≈ 0.25) but for random sampling fluctuations. We fitted this model on all data with t > 0 using a Beta distribution, as the issues raised for experimental data above regarding outliers did not apply (each data point here being the summarized outcome of 100 independent populations).

<u>- Front velocity</u>

In the long run, the position X_t of the front (i.e. the distance between the farthest populated patch and the release site) is expected to increase linearly with time, whether waves are pushed or pulled (e.g. Lewis et al., 2016):

$$X_t = v\, t$$

, where v is the asymptotic front velocity. However, expansions only settle on the velocity v after a transition period; the above equation is likely ill-suited for estimating front positions when

expansions are followed during their early stages and population sizes are low (so stochasticity is high). In these cases, which correspond to the present study, we propose to use the following model:

$$X_t = v_t t$$

$$v_t = v + (v_1 - v) \times e^{-\lambda_{[v]}(t-1)}$$

, where v_1 is the initial velocity after 1 generation of expansion (we use v_1 as our "starting point", and thus t – 1, because estimating velocities at t = 0 leads to convergence problems), and $\lambda_{[v]}$ the rate of exponential "decay" to the asymptotic velocity v.

We fitted this model to both simulated and experimental front locations, assuming a lognormal distribution to account for the fact distances travelled are always strictly positive (so we used only data with $t > 0$). For experimental data, the submodels for $\ln(v_1)$, $\ln(v)$ and $\log_{10}(\lambda_{[v]})$ included fixed effects for treatment as well as random effects of replicate identity. For simulated data, the submodel for v used logit(v) instead of $\ln(v)$, as velocities were by design ≤ 1, and the model was simplified by setting v_1 to 1. This is because given the initial population size at $t = 0$, all simulated landscapes were all but guaranteed to send at least one individual to the next patch during the first generation, (see **Fig. 1**), leading to a velocity of 1 at $t = 1$.

In simulations, the growth and dispersal functions are fully known, so we were also able to compare the estimated v to their respective v_F, the predicted velocity for a pulled wave with the same D_0 and r_0 (Birzu et al., 2019; the so-called "Fisherian velocity"; Lewis et al., 2016):

$$v_F = 2\sqrt{r_0 d_0}$$

, where $d_0 = 0.5\ D_0$ for a one-dimensional landscape with nearest neighbour dispersal (Birzu et al., 2019). Pulled waves are expected to have $\frac{v}{v_F} = 1$ (with some stochastic fluctuations), fully pushed waves to have $\frac{v}{v_F} \geq \frac{3}{2\sqrt{2}}$, and so-called semi-pushed waves to be in-between (Birzu et al., 2018, 2019). Because the formula we use for Allee effects leads to a fecundity of 0 (and a growth rate of $-\infty$) at density = 0, and because growth and dispersal at density = 0 are not meaningful anyway, we used r_1 and D_1 at $N = 1$ to estimate v_F rather than the "true" r_0 and D_0.

Results

Front velocity

In simulations, absolute asymptotic velocity of the front v differed between treatments: density-dependent dispersal led to higher velocities than in reference fronts, while Allee effects and reduced

connectivity fronts advanced slower (**Fig. 2**, **Supplementary Material 5**). Regarding relative velocities, reference fronts were very close to speeds expected for truly pulled waves (average velocity ratios $\frac{v}{v_F}$ = 1.01 and 0.99 for K = 450 and 225 respectively, **Fig. 2**); the other three treatments all had higher velocity ratios and were firmly in the range corresponding to true pushed waves (average velocity ratios $\frac{v}{v_F} \geq \frac{3}{2\sqrt{2}}$, **Fig. 2**). Fronts were faster when K = 450 than when K = 225 for all four treatments (**Fig. 2**, **Supplementary Material 5**).

By contrast, in experiments, front advances and absolute estimated asymptotic velocities were virtually indistinguishable between reference and "restricted connectedness" landscapes (**Fig. 3**). Similar results were found with other metrics such as the initial speed or the rate of convergence towards the asymptotic speed (**Supplementary Material 5**).

<u>Shifts in genetic diversity</u>

In simulations, genetic diversity declined faster, as measured by the decay rate λ, in front patches than in core patches for all treatments (**Fig. 4**, **Supplementary Material 5**). In both core and front patches, density-dependent dispersal and Allee effects led to a slower rate of diversity loss compared to the reference (**Fig. 4**, **Supplementary Material 5**). By contrast, reducing connectedness led to a faster rate of diversity loss (**Fig. 4**, **Supplementary Material 5**). In all four treatments and whether we looked at core or front patches, genetic diversity was lost faster when K = 225 than when K = 450 (**Fig. 4**, **Supplementary Material 5**).

In the experimental landscapes, genetic diversity also decayed on average in all tested contexts of our experiment (**Fig. 5**), and we also found differences between front and core patches and between both treatments. The rate of genetic diversity loss did not differ clearly between treatments in core patches (mean $\Delta_{\text{reference-restricted}} = -6.56 \times 10^{-3}$, 95% CI : [$-15.20 \times 10^{-3}$, 2.36×10^{-3}]), but was higher in reference fronts than in "reduced connectedness" fronts (mean $\Delta_{\text{reference-restricted}} = 18.70 \times 10^{-3}$, 95% CI : [$1.91 \times 10^{-3}$, 37.00×10^{-3}]) (**Fig. 5**, **Supplementary Material 5**). In addition, while expansion fronts lost diversity faster than core patches in reference landscapes, (mean $\Delta_{\text{front-core}} = 40.6 \times 10^{-3}$, 95% CI : [$27.8 \times 10^{-3}$, 54.3×10^{-3}]), this difference was reduced when connectedness was reduced (mean $\Delta_{\text{front-core}} = 15.4 \times 10^{-3}$, 95% CI : [$7.42 \times 10^{-3}$, 23.7×10^{-3}]) (**Fig. 5**).

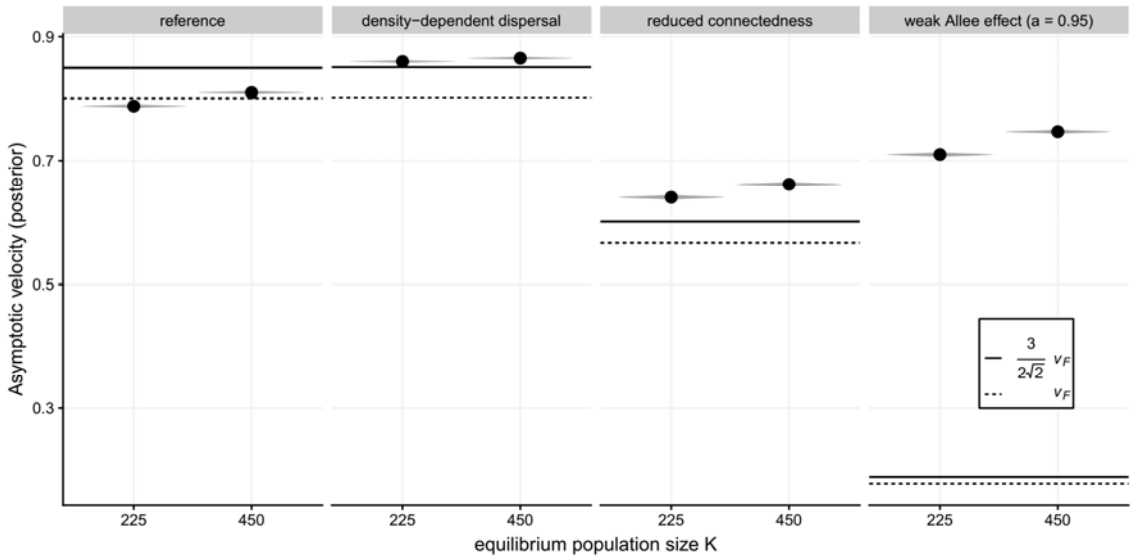

Figure 2. Posterior distribution of the asymptotic front velocity (v) in simulations, depending on simulation scenario and equilibrium population size K. The horizontal lines mark the range between $\frac{v}{v_F} = 1$ (i.e. pulled waves) and $\frac{v}{v_F} = \frac{3}{2\sqrt{2}}$ (limit between semi-pushed and fully pushed waves).

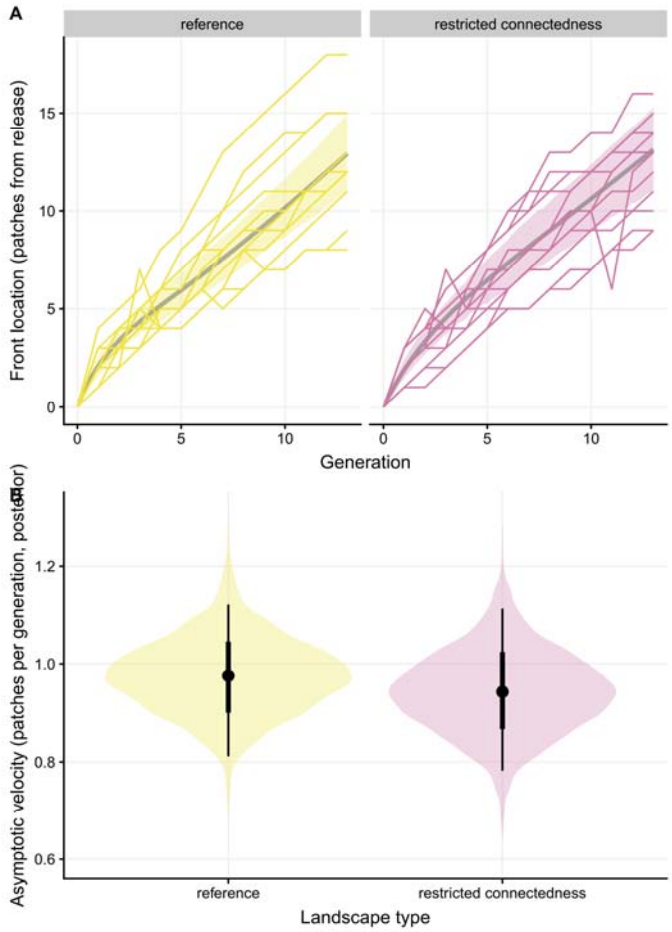

Figure 3. (A) Front locations as a function of the number of generations since release and experimental landscape type. Posterior means and 95% credible bands are displayed along observed trajectories for each landscape. (B) Posterior asymptotic velocity *v* as a function of landscape type.

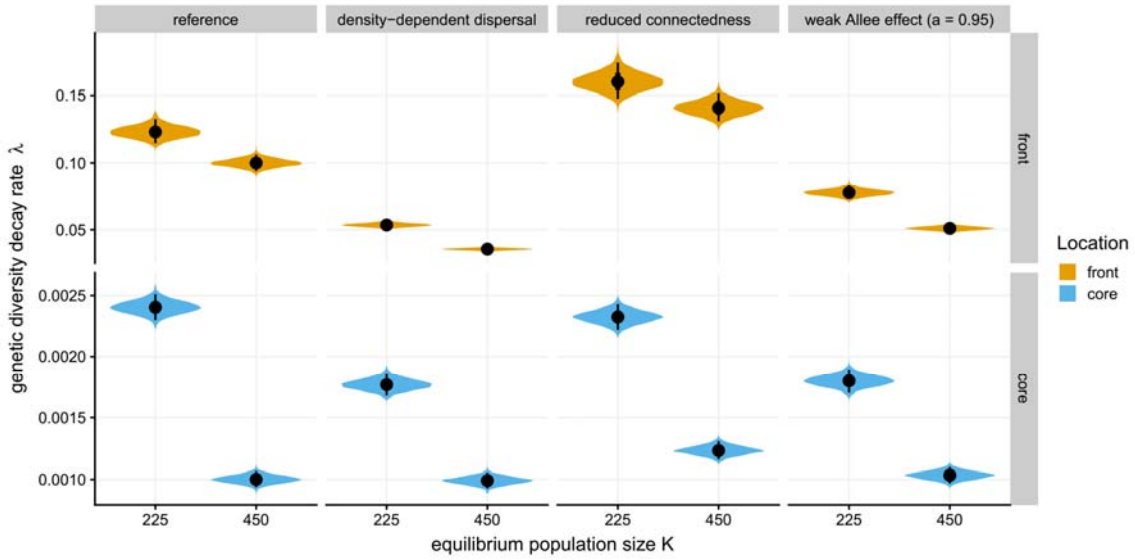

Figure 4. Posterior distribution of the decay rate of genetic with time (λ) in simulations, depending on simulation scenario, equilibrium population size K and patch location (either the original release site (core) or the most advanced patch at the time of measure (front)). Please note that posterior for core and front patches are displayed on different scales on the y-axis, for readability.

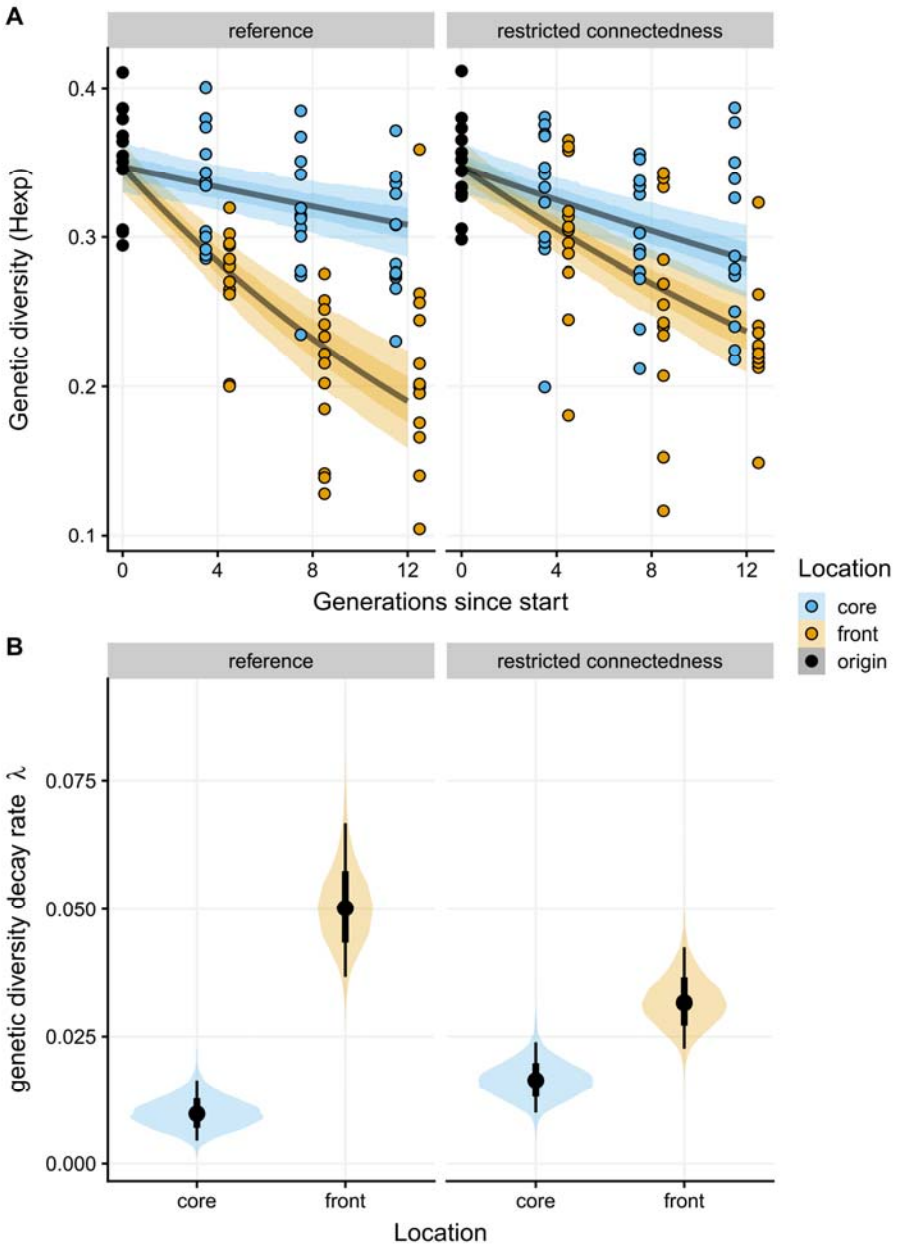

Figure 5. (A) Observed (points) and predicted (lines and bands) genetic diversity as a function of generations since release and landscape type. For predictions, lines are the posterior means and bands correspond to the 66/95% credible intervals. (B) Posterior distribution of the genetic diversity decay rate λ as a function of landscape type and patch location (either the original release site (core) or the most advanced patch at the time of measure (front).

Discussion

By combining an individual-based model and replicated range expansions in experimental landscapes, we showed that reducing connectedness can lead to pushed expansion waves.

Discrepancies between the simulation and experimental results, as well as comparisons between the different simulation treatments, potentially shed light on the mechanisms at play in each context.

<u>Front velocity as a quantitative and qualitative indicator of pushed waves</u>

First, our simulation results largely confirm previous theoretical and empirical results regarding the effects of density-dependent dispersal and Allee effects (Birzu et al., 2018, 2019; Gandhi et al., 2019, 2016; Hallatschek & Nelson, 2008; Roques et al., 2012). We show that both mechanisms lead to waves that can be classified as "pushed" based on the velocity ratio ($\frac{v}{v_F} \geq \frac{3}{2\sqrt{2}}$**; Fig. 2**), i.e. advancing faster than expected based on dispersal and growth at low densities. Genetic diversity is also lost at a slower rate in these waves compared to reference fronts (**Fig. 4**), confirming again previous results about pushed waves, which were however derived in landscapes with much larger population sizes, i.e. where drift and dispersal stochasticity were likely much less important. We also confirm that increasing the equilibrium population size K leads to faster range expansions (both in absolute terms and relative to the Fisher velocity), as previously shown by Haond et al. (2018).

In simulations, reducing connectedness also led to slower waves (lower absolute speed v) that were also pushed (higher velocity ratio $\frac{v}{v_F}$)(**Fig. 2).** Pushed waves arise when there is positive-density dependency in dispersal and/or growth at least at lower densities (Birzu et al., 2019; Gandhi et al., 2016; Haond et al., 2018; Lewis et al., 2016)**.** This result confirms our main prediction that the positive relationship between population density and establishment probability **(Fig. 1)** that arises at low population sizes due to stochasticity can be enough to generate pushed waves when connectedness declines.

In experimental landscapes, contrary to simulations, waves advanced just as fast when connectedness was reduced **(Fig. 3).** Importantly, it does not mean that reducing connectedness does not lead to more pushed waves, on the contrary. What differentiates between pushed and pulled waves is not absolute velocity v (which can be either higher or lower in pushed waves compared to the "equivalent" pulled waves, (Gandhi et al., 2019), **Fig. 2**), but velocity relative to the Fisherian velocity v_F. While we don't have direct information on the v_F of our experimental landscapes, we have some partial and indirect information. Indeed, while we do not know to what extent, a reduction of connectedness and thus dispersal (**Supplementary Material 3**) implies by definition a reduction of v_F, growth being equal. If $v_{[\text{reference}]} \approx v_{[\text{restricted}]}$ (**Fig. 3**) and $v_{F[\text{reference}]} > v_{F[\text{restricted}]}$, then it is likely that $v_{[\text{reference}]} / v_{F[\text{reference}]} < v_{[\text{restricted}]} / v_{F[\text{restricted}]}$, and that "restricted connectedness" fronts are indeed more pushed than reference fronts in our experiment. Our results thus show that full information about the density-dependency of growth or movement is not always

needed to make qualitative assessments of the pushed or pulled nature of a given expansion wave relative to a reference. This is particularly interesting for the study of biological invasions and range shifts in the wild, especially in (larger) organisms that are not easily reared and maintained in laboratory conditions. More work is needed to determine whether more quantitative insights about the pushed or pulled nature of expansion waves can also be obtained from incomplete life-history and population dynamics data typical of "natural" study systems.

Mismatches to genetic diversity predictions show pushed waves are more diverse than expected

A key theoretical prediction is that pushed waves lose genetic diversity at a slower rate than comparable pulled waves (Birzu et al., 2019; Hallatschek & Nelson, 2008; Roques et al., 2012). While our simulated pushed waves generated by density-dependent dispersal or Allee effects conform to this prediction **(Fig. 4),** this is not the case for simulated waves we generated by reducing connectedness: these expansion fronts lost genetic diversity slightly faster than the pulled reference **(Fig. 4)** despite being clearly "pushed" based on velocity ratios. This conflict between two definitions of pushed waves is at first glance surprising, as previous theory tended to imply they were intrinsically correlated (e.g. Birzu et al., 2018). We propose this result is driven by the way stochasticity interacts with dispersal probability at "low" population sizes to determine, not only establishment probability (**Fig. 1**), but also the number of individuals founding a new population. Intuitively, reducing the dispersal rate reduces the *absolute* average number of individuals that can start new populations (**Supplementary Material 6**), likely leading to lower effective population sizes and thus a faster decay of genetic diversity (Birzu et al., 2018, 2019; Hallatschek & Nelson, 2008). However, because of stochasticity-induced failures, the *relative* number of individuals contributing to a new population (that is, compared to what would expect assuming deterministic dispersal) is higher when connectedness is reduced (**Supplementary Material 6)**. That is, we can reconcile our simulated results with theory by noting that, compared to a hypothetical case where average dispersal is reduced with no corresponding increase in stochasticity, reducing connectedness does lead to higher population sizes, and probably lower genetic diversity loss as expected for pushed waves. The caveat is that, in any case, this is not enough to compensate for the simple and direct effect of reducing dispersal on (effective) population sizes.

In experimental landscapes, reducing connectivity did slow the decay of genetic diversity at the front (**Fig. 5**), as was expected from pushed wave theory (Birzu et al., 2018, 2019; Gandhi et al., 2019; Roques et al., 2012). However, as seen above, this result contradicts simulations showing "pushed" waves arising solely because of reduced connectedness should lose genetic diversity faster than the equivalent wave with higher connectedness. The mismatch between simulations and experiments

regarding genetic diversity indicates increased stochasticity is not the only mechanism at play here. Dispersal decisions depend on the balance between costs and benefits of both dispersal and philopatry. While reducing connectedness increases the costs of dispersal (Bonte et al., 2012), leading to a decrease in dispersal (Benoit et al., 2020; Bonte et al., 2012), this effect may be weaker at higher densities, if costs associated with competition are strong enough to trigger dispersal anyway. In that context, reduced connectedness would strengthen the density-dependency of dispersal, leading to more pushed waves through another mechanism. This verbal prediction is anecdotally supported by some theoretical and simulation results, where the difference in dispersal between contexts with high and low costs of dispersal is reduced at higher densities (Henriques-Silva, Boivin, Calcagno, Urban, & Peres-Neto, 2015; Poethke & Hovestadt, 2002). To test this hypothesis, we implemented this it in further range expansion simulations (**Supplementary Material 7**), adding a treatment combining restricted base dispersal and positive density-dependent dispersal at the same time. This treatment, in which dispersal at higher densities close to *K* is more or less the same than in reference fronts, results in simulated waves that match our experiment better. Indeed, the resulting waves (i) are pushed based on velocity ratios (ii) have an absolute speed closer to reference fronts than when only restricted connectedness is applied, and (iii) lose genetic diversity slower. For this mechanism to plausibly apply to our experimental system, *Trichogramma* wasps would need to be able to detect when density and competition for hosts increase in their current patch, and adjust their spatial behaviour in response. Literature on host choice shows that they are indeed able to do so, and are more likely to leave patches where too many eggs have already been parasitized (Wajnberg, Fauvergue, & Pons, 2000).

Alternatively, experimental landscapes with restricted connectedness may lose genetic diversity more slowly simply because they exhibit larger populations, rather than due to a shift in regime from (more) pulled to (more) pushed waves. While we do find larger population sizes in core populations when connectedness is restricted **(Supplementary Material 8),** we do not believe it is the main driver of our genetic diversity results, for at least two reasons. First, the relative difference diversity loss between reference and "restricted connectedness" fronts in experiments is higher than between simulated fronts with K = 225 versus K = 450 (compare **Figs. 4** and **5**). In experiments, restricting connectedness only increased population sizes by about 20% (**Supplementary Material 8**). Second and more importantly, if the differences in genetic dynamics at the front were mostly due to differences in carrying capacities, we should then expect similar dynamics in core populations, at least qualitatively (see simulated results **Fig. 4**). This is not the case, as genetic decay rates are not different between treatments in experimental core patches (**Fig. 5**).

Conclusion

In this study, we demonstrated that pushed and pulled-like wave dynamics can be detected and analysed even in systems with (relatively) low population sizes, despite theoretical tools being developed assuming much higher population sizes. This means these tools have the potential to be useful in a much broader range of contexts and taxa, and may be extremely valuable to help us understand and better predict range expansions and shifts under natural conditions. We also demonstrated a new mechanism for generating pushed(-like) waves that can only arise at "lower" population sizes **(Fig. 1).** We show the genetic and velocity aspects of the pushed/pulled distinction, which have been implied to be tightly linked (Birzu et al., 2018) can be decoupled under these contexts. This is not without precedent, as similar results have been found regarding front width and velocity (Gandhi et al., 2016). This means (empirical) researchers looking to analyse range expansions under the pushed/pulled lens must be careful about which questions they ask and whether the types of data they collect are appropriate. One cannot assume one dimension/metric of "pushiness" is necessarily correlated with the others, especially when the focal species have small population sizes (here, "small" can be operationally defined as "small enough that the effects described in **Fig. 1** apply at the low-density wavefront"). More generally, this shows more studies are needed to understand these types of "partially" pushed waves and their impacts.

Finally, our experimental results show that, in some cases, reducing connectivity may increase population sizes and limit the loss of genetic diversity while not substantially impeding spread rates. This leads to the somewhat counterintuitive conclusion that reducing connectivity may in some cases benefit expanding species (compare and contrast with e.g. Hodgson, Thomas, Dytham, Travis, & Cornell, 2012; Kinezaki, Kawasaki, & Shigesada, 2010). Given positive density-dependent dispersal, a main cause of pushed waves, occurs frequently (see syntheses in Harman et al., 2020; Matthysen, 2005), this has strong implications for the management of invasive species and species undergoing range shifts. Also, as density-dependent dispersal (E. A. Fronhofer, Gut, & Altermatt, 2017; Travis, Mustin, Benton, & Dytham, 2009) and Allee effects (Datta, Korolev, Cvijovic, Dudley, & Gore, 2013; Erm & Phillips, 2019) themselves may well evolve during range expansions, and given the consequences of habitat fragmentation on dispersal ecology and evolution (Cote et al., 2017; Jacob, Laurent, Morel-Journel, & Schtickzelle, 2020; Travis, Smith, & Ranwala, 2010), we call for more systematic eco-evolutionary studies of context-dependent dynamics during range expansion and shifts.

Acknowledgements

We thank participants to the 2019 conference of the British Ecological Society for their insightful comments.

Data availability

Data, Netlogo model code and R scripts to reproduce all analyses presented in this manuscript will be available on Github and Zenodo starting with the next update of this manuscript.

Funding

This work was funded by the French Agence Nationale de la Recherche (TriPTIC, ANR-14-CE18-0002; PushToiDeLa, ANR-18-CE32-0008).

References

Baudry, J., & Merriam, H. G. (1987). Connectivity and connectedness: functional versus structural patterns in landscapes. In K.-F. Schreiber (Ed.), *Connectivity in Landscape Ecology* (pp. 23–28). Münster.

Benoit, L., Hewison, A. J. M., Coulon, A., Debeffe, L., Grémillet, D., Ducros, D., … Morellet, N. (2020). Accelerating across the landscape: The energetic costs of natal dispersal in a large herbivore. *Journal of Animal Ecology*, *89*(1), 173–185. doi: 10.1111/1365-2656.13098

Berec, L., Angulo, E., & Courchamp, F. (2007). Multiple Allee effects and population management. *Trends in Ecology & Evolution*, *22*(4), 185–191. doi: 10.1016/j.tree.2006.12.002

Birzu, G., Hallatschek, O., & Korolev, K. S. (2018). Fluctuations uncover a distinct class of traveling waves. *Proceedings of the National Academy of Sciences*, *115*(16), E3645–E3654. doi: 10.1073/pnas.1715737115

Birzu, G., Matin, S., Hallatschek, O., & Korolev, K. S. (2019). Genetic drift in range expansions is very sensitive to density dependence in dispersal and growth. *Ecology Letters*, *22*(11), 1817–1827. doi: 10.1111/ele.13364

Bonte, D., Van Dyck, H., Bullock, J. M., Coulon, A., Delgado, M., Gibbs, M., … Travis, J. M. J. (2012). Costs of dispersal. *Biological Reviews*, *87*(2), 290–312. doi: 10.1111/j.1469-185X.2011.00201.x

Bowler, D. E., & Benton, T. G. (2005). Causes and consequences of animal dispersal strategies: relating individual behaviour to spatial dynamics. *Biological Reviews*, *80*(2), 205–225. doi: 10.1017/S1464793104006645

Bürkner, P.-C. (2017). brms: an R package for bayesian multilevel models using Stan. *Journal of Statistical Software*, *80*(1), 1–28. doi: 10.18637/jss.v080.i01

Carpenter, B., Gelman, A., Hoffman, M. D., Lee, D., Goodrich, B., Betancourt, M., … Riddell, A. (2017). Stan: a probabilistic programming language. *Journal of Statistical Software*, *76*(1), 1–32. doi: 10.18637/jss.v076.i01

Cerutti, F., & Bigler, F. (1995). Quality assessment of *Trichogramma brassicae* in the laboratory. *Entomologia Experimentalis et Applicata*, *75*(1), 19–26. doi: 10.1111/j.1570-7458.1995.tb01905.x

Cote, J., Bestion, E., Jacob, S., Travis, J., Legrand, D., & Baguette, M. (2017). Evolution of dispersal strategies and dispersal syndromes in fragmented landscapes. *Ecography*, *40*(1), 56–73. doi: 10.1111/ecog.02538

Datta, M. S., Korolev, K. S., Cvijovic, I., Dudley, C., & Gore, J. (2013). Range expansion promotes cooperation in an experimental microbial metapopulation. *Proceedings of the National Academy of Sciences*, *110*(18), 7354–7359. doi: 10.1073/pnas.1217517110

De Meester, N., & Bonte, D. (2010). Information use and density-dependent emigration in an agrobiont spider. *Behavioral Ecology*, *21*(5), 992–998. doi: 10.1093/beheco/arq088

DeAngelis, D. L., & Mooij, W. M. (2005). Individual-based modeling of ecological and evolutionary processes. *Annual Review of Ecology, Evolution, and Systematics*, *36*, 147–168.

Endriss, S. B., Vahsen, M. L., Bitume, E. V., Monroe, J. G., Turner, K. G., Norton, A. P., & Hufbauer, R. A. (2019). The importance of growing up: juvenile environment influences dispersal of individuals and their neighbours. *Ecology Letters*, *22*(1), 45–55. doi: 10.1111/ele.13166

Erm, P., & Phillips, B. L. (2019). Evolution transforms pushed waves into pulled waves. *The American Naturalist*. doi: 10.1086/707324

Facon, B., Genton, B. J., Shykoff, J., Jarne, P., Estoup, A., & David, P. (2006). A general eco-evolutionary framework for understanding bioinvasions. *Trends in Ecology & Evolution*, *21*(3), 130–135. doi: 10.1016/j.tree.2005.10.012

Fronhofer, E. A., Gut, S., & Altermatt, F. (2017). Evolution of density-dependent movement during experimental range expansions. *Journal of Evolutionary Biology*, *30*(12), 2165–2176. doi: 10.1111/jeb.13182

Fronhofer, Emanuel A., Legrand, D., Altermatt, F., Ansart, A., Blanchet, S., Bonte, D., … Cote, J. (2018). Bottom-up and top-down control of dispersal across major organismal groups. *Nature Ecology & Evolution*, *2*(12), 1859. doi: 10.1038/s41559-018-0686-0

Gabry, J., Simpson, D., Vehtari, A., Betancourt, M., & Gelman, A. (2019). Visualization in Bayesian workflow. *Journal of the Royal Statistical Society: Series A (Statistics in Society)*, *182*(2), 389–402. doi: 10.1111/rssa.12378

Gandhi, S. R., Korolev, K. S., & Gore, J. (2019). Cooperation mitigates diversity loss in a spatially expanding microbial population. *Proceedings of the National Academy of Sciences*, *116*(47), 23582–23587. doi: 10.1073/pnas.1910075116

Gandhi, S. R., Yurtsev, E. A., Korolev, K. S., & Gore, J. (2016). Range expansions transition from pulled to pushed waves as growth becomes more cooperative in an experimental microbial population. *Proceedings of the National Academy of Sciences*, *113*(25), 6922–6927. doi: 10.1073/pnas.1521056113

Hallatschek, O., & Nelson, D. R. (2008). Gene surfing in expanding populations. *Theoretical Population Biology*, *73*(1), 158–170. doi: 10.1016/j.tpb.2007.08.008

Haond, M., Morel-Journel, T., Lombaert, E., Vercken, E., Mailleret, L., & Roques, L. (2018). When higher carrying capacities lead to faster propagation. *BioRxiv (Peer-Reviewed and Recommended by Peer Community In Ecology)*, 307322. doi: 10.1101/307322

Harman, R. R., Ii, J. G., Shivaji, R., & Cronin, J. T. (2020). Frequency of occurrence and population-dynamic consequences of different forms of density-dependent emigration. *The American Naturalist*. doi: 10.1086/708156

Hastings, A., Cuddington, K., Davies, K. F., Dugaw, C. J., Elmendorf, S., Freestone, A., … Thomson, D. (2005). The spatial spread of invasions: new developments in theory and evidence. *Ecology Letters*, *8*(1), 91–101. doi: 10.1111/j.1461-0248.2004.00687.x

Henriques-Silva, R., Boivin, F., Calcagno, V., Urban, M. C., & Peres-Neto, P. R. (2015). On the evolution of dispersal via heterogeneity in spatial connectivity. *Proceedings of the Royal Society B: Biological Sciences*, *282*(1803), 20142879. doi: 10.1098/rspb.2014.2879

Hill, J. K., Griffiths, H. M., & Thomas, C. D. (2011). Climate change and evolutionary adaptations at species' range margins. *Annual Review of Entomology*, *56*(1), 143–159. doi: 10.1146/annurev-ento-120709-144746

Hodgson, J. A., Thomas, C. D., Dytham, C., Travis, J. M. J., & Cornell, S. J. (2012). The speed of range shifts in fragmented landscapes. *PLOS ONE*, *7*(10), e47141. doi: 10.1371/journal.pone.0047141

Hovestadt, T., Kubisch, A., & Poethke, H.-J. (2010). Information processing in models for density-dependent emigration: A comparison. *Ecological Modelling*, *221*(3), 405–410. doi: 10.1016/j.ecolmodel.2009.11.005

Jacob, S., Chaine, A. S., Huet, M., Clobert, J., & Legrand, D. (2019). Variability in dispersal syndromes is a key driver of metapopulation dynamics in experimental microcosms. *The American Naturalist*, *194*(5), 613–626. doi: 10.1086/705410

Jacob, S., Laurent, E., Morel-Journel, T., & Schtickzelle, N. (2020). Fragmentation and the context-dependence of dispersal syndromes: matrix harshness modifies resident-disperser phenotypic differences in microcosms. *Oikos*, *129*(2), 158–169. doi: 10.1111/oik.06857

Jombart, T. (2008). adegenet: a R package for the multivariate analysis of genetic markers. *Bioinformatics*, *24*(11), 1403–1405. doi: 10.1093/bioinformatics/btn129

Kay, M. (2019). *tidybayes: Tidy Data and Geoms for Bayesian Models*. doi: 10.5281/zenodo.1308151

Kinezaki, N., Kawasaki, K., & Shigesada, N. (2010). The effect of the spatial configuration of habitat fragmentation on invasive spread. *Theoretical Population Biology*, *78*(4), 298–308. doi: 10.1016/j.tpb.2010.09.002

Krauss, J., Steffan-Dewenter, I., & Tscharntke, T. (2003). How does landscape context contribute to effects of habitat fragmentation on diversity and population density of butterflies? *Journal of Biogeography*, *30*(6), 889–900. doi: 10.1046/j.1365-2699.2003.00878.x

Kruschke, J. (2015). *Doing Bayesian Data Analysis: A Tutorial with R, JAGS, and Stan* (2nd ed.). Boston: Academic Press.

Kuefler, D., Avgar, T., & Fryxell, J. M. (2012). Rotifer population spread in relation to food, density and predation risk in an experimental system: *State-dependent rate of population spread*. *Journal of Animal Ecology*, *81*(2), 323–329. doi: 10.1111/j.1365-2656.2011.01917.x

Larsen, C. D., & Hargreaves, A. L. (2020). Miniaturizing landscapes to understand species distributions. *Ecography*, *43*(n/a). doi: 10.1111/ecog.04959

Lavergne, S., Mouquet, N., Thuiller, W., & Ronce, O. (2010). Biodiversity and climate change: integrating evolutionary and ecological responses of species and communities. *Annual Review of Ecology, Evolution, and Systematics*, *41*(1), 321–350. doi: 10.1146/annurev-ecolsys-102209-144628

Lewis, M., Petrovskii, S. V., & Potts, J. (2016). *The Mathematics Behind Biological Invasions*. doi: 10.1007/978-3-319-32043-4

Marjamäki, P. H., Contasti, A. L., Coulson, T. N., & McLoughlin, P. D. (2013). Local density and group size interacts with age and sex to determine direction and rate of social dispersal in a polygynous mammal. *Ecology and Evolution*, *3*(9), 3073–3082. doi: 10.1002/ece3.694

Matthysen, E. (2005). Density-dependent dispersal in birds and mammals. *Ecography*, *28*(3), 403–416.

McElreath, R. (2020). *Statistical Rethinking: A Bayesian Course with Examples in R and Stan* (2nd edition). Boca Raton: Chapman and Hall/CRC.

Minto, C., Myers, R. A., & Blanchard, W. (2008). Survival variability and population density in fish populations. *Nature*, *452*(7185), 344–347. doi: 10.1038/nature06605

Morel-Journel, T., Girod, P., Mailleret, L., Auguste, A., Blin, A., & Vercken, E. (2016). The highs and lows of dispersal: how connectivity and initial population size jointly shape establishment dynamics in discrete landscapes. *Oikos*, *125*(6), 769–777. doi: 10.1111/oik.02718

Nei, M. (1973). Analysis of gene diversity in subdivided populations. *Proceedings of the National Academy of Sciences*, *70*(12), 3321–3323. doi: 10.1073/pnas.70.12.3321

Pachepsky, E., & Levine, J. M. (2011). Density Dependence Slows Invader Spread in Fragmented Landscapes. *The American Naturalist*, *177*(1), 18–28. doi: 10.1086/657438

Parmesan, C. (2006). Ecological and evolutionary responses to recent climate change. *Annual Review of Ecology, Evolution, and Systematics*, *37*(1), 637–669. doi: 10.1146/annurev.ecolsys.37.091305.110100

Pedersen, T. L. (2019). *patchwork: The Composer of Plots*. Retrieved from https://CRAN.R-project.org/package=patchwork

Poethke, H. J., & Hovestadt, T. (2002). Evolution of density–and patch–size–dependent dispersal rates. *Proceedings of the Royal Society of London B: Biological Sciences*, *269*(1491), 637–645. doi: 10.1098/rspb.2001.1936

R Core Team. (2020). R: a language and environment for statistical computing (Version 3.6.3). Retrieved from https://www.R-project.org/

Renault, D., Laparie, M., McCauley, S. J., & Bonte, D. (2018). Environmental adaptations, ecological filtering, and dispersal central to insect invasions. *Annual Review of Entomology*, *63*(1), 345–368. doi: 10.1146/annurev-ento-020117-043315

Roques, L., Garnier, J., Hamel, F., & Klein, E. K. (2012). Allee effect promotes diversity in traveling waves of colonization. *Proceedings of the National Academy of Sciences*, *109*(23), 8828–8833. doi: 10.1073/pnas.1201695109

Salecker, J., Sciaini, M., Meyer, K. M., & Wiegand, K. (2019). The nlrx r package: A next-generation framework for reproducible NetLogo model analyses. *Methods in Ecology and Evolution*, *10*(11), 1854–1863. doi: 10.1111/2041-210X.13286

Santini, L., Isaac, N. J. B., & Ficetola, G. F. (2018). TetraDENSITY: A database of population density estimates in terrestrial vertebrates. *Global Ecology and Biogeography*, *27*(7), 787–791. doi: 10.1111/geb.12756

Sexton, J. P., McIntyre, P. J., Angert, A. L., & Rice, K. J. (2009). Evolution and ecology of species range limits. *Annual Review of Ecology, Evolution, and Systematics*, *40*(1), 415–436. doi: 10.1146/annurev.ecolsys.110308.120317

Stan Development Team. (2018). RStan: the R interface to Stan (Version 2.17.3). Retrieved from http://mc-stan.org

Stephens, P. A., Vieira, M. V., Willis, S. G., & Carbone, C. (2019). The limits to population density in birds and mammals. *Ecology Letters*, *22*(4), 654–663. doi: 10.1111/ele.13227

Stevens, V. M., Trochet, A., Blanchet, S., Moulherat, S., Clobert, J., & Baguette, M. (2013). Dispersal syndromes and the use of life-histories to predict dispersal. *Evolutionary Applications*, *6*(4), 630–642. doi: 10.1111/eva.12049

Stokes, A. N. (1976). On two types of moving front in quasilinear diffusion. *Mathematical Biosciences*, *31*(3), 307–315. doi: 10.1016/0025-5564(76)90087-0

St-Onge, M., Cormier, D., Todorova, S., & Lucas, É. (2014). Comparison of *Ephestia* kuehniella eggs sterilization methods for *Trichogramma* rearing. *Biological Control*, *70*, 73–77. doi: 10.1016/j.biocontrol.2013.12.006

Travis, J. M. J., Mustin, K., Benton, T. G., & Dytham, C. (2009). Accelerating invasion rates result from the evolution of density-dependent dispersal. *Journal of Theoretical Biology*, *259*(1), 151–158. doi: 10.1016/j.jtbi.2009.03.008

Travis, J. M. J., Smith, H. S., & Ranwala, S. M. W. (2010). Towards a mechanistic understanding of dispersal evolution in plants: conservation implications. *Diversity and Distributions*, *16*(4), 690–702. doi: 10.1111/j.1472-4642.2010.00674.x

Van Allen, B. G., & Bhavsar, P. (2014). Natal habitat effects drive density—dependent scaling of dispersal decisions. *Oikos*, *123*(6), 699–704. doi: 10.1111/oik.01240

Van Petegem, K., Moerman, F., Dahirel, M., Fronhofer, E. A., Vandegehuchte, M. L., Van Leeuwen, T., … Bonte, D. (2018). Kin competition accelerates experimental range expansion in an arthropod herbivore. *Ecology Letters*, *21*(2), 225–234. doi: 10.1111/ele.12887

Vehtari, A., Gelman, A., Simpson, D., Carpenter, B., & Bürkner, P.-C. (2020). Rank-normalization, folding, and localization: An improved \widehat{R} for assessing convergence of MCMC. *ArXiv:1903.08008 [Stat]*. Retrieved from http://arxiv.org/abs/1903.08008

Wajnberg, E., Fauvergue, X., & Pons, O. (2000). Patch leaving decision rules and the Marginal Value Theorem: an experimental analysis and a simulation model. *Behavioral Ecology*, *11*(6), 577–586. doi: 10.1093/beheco/11.6.577

Walter, J. A., Grayson, K. L., Blackburn, L. M., Tobin, P. C., & Johnson, D. M. (2019). Spatiotemporal variability in Allee effects of invading gypsy moth populations. *Biological Invasions*. doi: 10.1007/s10530-019-02096-5

Wickham, H., Averick, M., Bryan, J., Chang, W., McGowan, L., François, R., … Yutani, H. (2019). Welcome to the Tidyverse. *Journal of Open Source Software*, *4*(43), 1686. doi: 10.21105/joss.01686

Wilensky, U. (1999). *NetLogo*. Retrieved from http://ccl.northwestern.edu/netlogo/

Williams, J. L., & Levine, J. M. (2018). Experimental evidence that density dependence strongly influences plant invasions through fragmented landscapes. *Ecology*, *99*(4), 876–884. doi: 10.1002/ecy.2156

686 Tables

687 **Table 1:** Values of key parameters of the individual-based model used to simulate range expansions,
688 for the four scenarios considered in the present study. Values that differ from the reference are in
689 **bold**.

Parameter name and description	Value in scenario :			
	reference	density-dependent dispersal	(weak) Allee effect	reduced connectivity
K : equilibrium population size	225 or 450	225 or 450	225 or 450	225 or 450
r_0: growth rate at N = 0 (in the absence of Allee effects)	ln(5)	ln(5)	ln(5)	ln(5)
D_0: dispersal rate at N = 0	0.2	0.2	0.2	**0.1**
$\beta_{density}$: slope of the dispersal-density relationship (logit scale)	0	**1**	0	0
A : Allee effect parameter	0	0	**0.95**	0

690

691